DOI: 10.1002/chem.200902346

A Flexible Pro-porous Coordination Polymer: Non-conventional Synthesis and Separation Properties Towards CO_2/CH_4 Mixtures

Elisa Barea,[a] Giulia Tagliabue,[a, b] Wen-Guo Wang,[a] Manuel Pérez-Mendoza,[a] Laura Mendez-Liñan,[a] Francisco J. López-Garzon,[a] Simona Galli,*[b] Norberto Masciocchi,[b] and Jorge A. R. Navarro*[a]

Abstract: The novel coordination polymers $[Cu(Hoxonic)(H_2O)]_n$ (**1**) and $[Cu(Hoxonic)(bpy)_{0.5}]_n \cdot 1.5n\,H_2O$ (**2⊃H_2O**) (H_3oxonic: 4,6-dihydroxy-1,3,5-triazine-2-carboxylic acid; bpy: 4,4′-bipyridine) have been isolated and structurally characterised by ab initio X-ray powder diffraction. The dense phase **1** contains 1D zig-zag chains in which Hoxonic dianions bridge square-pyramidal copper(II) ions, apically coordinated by water molecules. On the contrary, **2⊃H_2O**, prepared by solution and solventless methods, is based on 2D layers of octahedral copper(II) ions bridged by Hoxonic ligands, further pillared by bpy spacers. The resulting pro-porous 3D network possesses small hydrated cavities. The reactivity, thermal, magnetic and adsorptive properties of these materials have been investigated. Notably, the adsorption studies on **2** show that this material possesses unusual adsorption behaviour. Indeed, guest uptake is facilitated by increasing the thermal energy of both the guest and the framework. Thus, neither N_2 at 77 K nor CO_2 at 195 K are incorporated, and CH_4 is only minimally adsorbed at 273 K and high pressures (0.5 mmol g^{-1} at 2500 kPa). By contrast, CO_2 is readily incorporated at 273 K (up to 2.5 mmol g^{-1} at 2500 kPa). The selectivity of **2** towards CO_2 over CH_4 has been investigated by means of variable-temperature zero coverage adsorption experiments and measurement of breakthrough curves of CO_2/CH_4 mixtures. The results show the highly selective incorporation of CO_2 in **2**, which can be rationalised on the basis of the framework flexibility and polar nature of its voids.

Keywords: carbon dioxide capture · gas separation · metal–organic frameworks · methane purification · thermochemistry

Introduction

The highly tuneable porous structure of metal organic frameworks (MOFs) or porous coordination polymers (PCPs)[1] offers the possibility of performing technologically relevant processes in an extremely selective way. Examples of selective adsorptive features,[2] separation processes[3] and catalysis[4] for this kind of materials can readily be found in the literature. In this regard, framework flexibility is one of the most desirable features in order to achieve these processes in a highly specific way.[5,6]

With the aim of fine tuning the structural and functional features of novel PCPs, our group is making use of differently substituted pyrimidines [that is, pyrimidine-4-olate (4-pymo), 5-X-pyrimidine-2-olate (5-Xpymo; X = H, F, Cl, Br, I, NO_2), pyrimidine-4,6-dicarboxylate (pmdc)] in combination with first and second row transition metal ions allowing the isolation of numerous functional, dense[7] as well as porous,[8] 3D materials. The latter, with unusually high thermal and chemical stabilities, possess flexible porous frameworks toward probe gases, this aspect favouring their remarkable storage abilities towards industrially and environmentally relevant gases.[8,9]

Following our previous results, we reacted the potassium salt of the 4,6-dihydroxy-1,3,5-triazine-2-carboxylic acid

[a] Dr. E. Barea, G. Tagliabue, Dr. W.-G. Wang, Dr. M. Pérez-Mendoza, L. Mendez-Liñan, Prof. F. J. López-Garzon, Prof. J. A. R. Navarro
Departamento de Química Inorgánica
Universidad de Granada, Av. Fuentenueva S/N
18071 Granada (Spain)
Fax: (+34) 958-248526
E-mail: jarn@ugr.es

[b] G. Tagliabue, Dr. S. Galli, Prof. N. Masciocchi
Dipartimento di Scienze Chimiche e Ambientali
Università degli Studi dell'Insubria
Via Valleggio 11, 22100 Como (Italy)
Fax: (+39) 031-2386630
E-mail: simona.galli@uninsubria.it

Supporting information for this article is available on the WWW under http://dx.doi.org/10.1002/chem.200902346.

(KH_2oxonic) with copper(II) salts, obtaining the dense $[Cu(Hoxonic)(H_2O)]_n$ species (**1**), based on 1D chains. **1** can be further reacted with rod like *N,N'* ligands to yield the 3D pro-porous framework $[Cu(Hoxonic)(bpy)_{0.5}]_n \cdot 1.5n\,H_2O$ (**2⊂H$_2$O**; bpy: 4,4′-bipyridine) (Scheme 1). Thus, in this contribution, we report on the synthesis, the crystal structure, the thermal behaviour and the magnetic properties of **1** and **2⊂H$_2$O**. Finally, the adsorptive properties of the activated system $[Cu(Hoxonic)(bpy)_{0.5}]_n$ (**2**) have been studied in detail, revealing an unusual behaviour, which can be rationalised on the basis of its pro-porous flexible framework. We also show that the adsorptive properties of this system are useful for the selective removal of CO_2 by adsorption from CO_2/CH_4 mixtures.

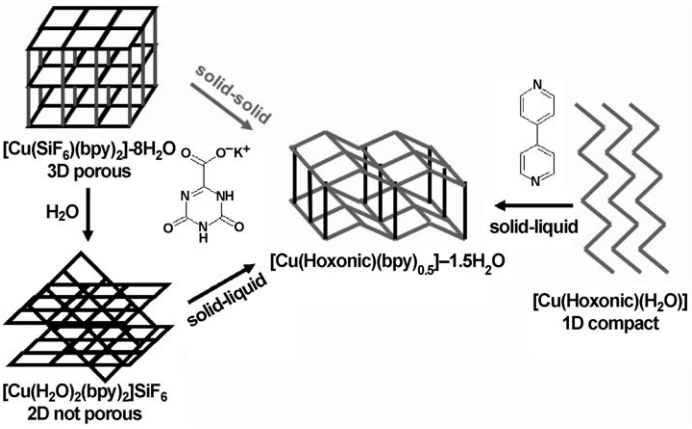

Scheme 1. Different synthetic strategies leading to compound **2⊂H$_2$O**.

Results and Discussion

Synthesis: $[Cu(Hoxonic)(H_2O)]_n$ (**1**) was isolated by following a straightforward synthetic procedure, reacting, in aqueous medium, copper(II) perchlorate with the potassium salt of the oxonic acid. Its structure determination (see below) highlighted that it is composed of 1D chains. As such, **1** appeared as a good building block for the construction of multidimensional architectures, provided that the 1D chains could be joined together with suitable ligands in order to obtain pillared networks with large channels.[10] With this purpose, having the building-block approach in mind, we reacted compound **1** with *N,N'*-rod like ligands of different length and flexibility (pyrazine, 4,4′-bipyridine, 1,2-bis(4-pyridyl)-ethane, *trans*-1,2-di-(4-pyridyl)-ethylene and bis-(4-pyridyl)-acetylene): in the case of 4,4′-bipyridine, we successfully isolated a microcrystalline compound formulated as $[Cu(Hoxonic)(bpy)_{0.5}]_n \cdot 1.5n\,H_2O$ (**2⊂H$_2$O**) (Scheme 1). We then explored other, conventional or non conventional, synthetic strategies. The results show that the formation of the $[Cu(Hoxonic)(bpy)_{0.5}]_n \cdot 1.5n\,H_2O$ system is favoured not only by a solid-liquid reaction involving solid $[Cu(Hoxonic)(H_2O)]_n$ and a methanolic solution of bpy, but also: i) by a conventional one-pot solid-liquid reaction involving a copper salt and the two Hoxonic and bpy ligands as starting materials; ii) by the reaction of the KH_2oxonic salt with different Kitagawa's Cu/bpy coordination polymers[11] through different reaction paths (see Scheme 1 and the Experimental Section).

Thermal behaviour: The thermal behaviour of compounds **1** and **2⊂H$_2$O** was investigated by coupling in situ variable-temperature X-ray powder diffraction (TXRPD) and simultaneous thermal analyses (STA, that is, simultaneous TG and DSC).

*$[Cu(Hoxonic)(H_2O)]_n$ (**1**)*: The simultaneous thermal analysis performed on compound **1** (Figure S1) showed no mass loss from 303 K up to 513 K, when the decomposition process starts. The residual mass after decomposition completion at 1073 K accounts for the formation of Cu_2O, the stable copper oxide phase at high temperatures. The TXRPD experiments carried out in air on **1** (Figure 1a) further substantiated the STA observations (Figure S1): progressive heating up to decomposition only affected the cell parameters. Although *b* and β remain practically constant over the investigated temperature range, *a* and *c* slightly increase, promoting a modest cell volume increment of about 1.4% (Figure 1b). As evident from Figure 1c, showing the representation of the thermal strain tensor, on the whole heating brings about a clearly anisotropic structure expansion, the less pronounced changes being observed along the direction of stacking, .[10–1]

As appreciable from Figure 1a, no phase changes could be detected. In this regard, it is noteworthy that the thermal treatment does not lead to dehydration. The unexpected lack of dehydration was confirmed by repeated STA and TXRPD experiments. As a further proof, Rietveld refinements were carried out on the variable-temperature data refining the water oxygen site occupation factor: the presence of one water molecule per asymmetric unit was invariably proved at any temperature (Figure S2). The unusual stability of the hydrated form may be tentatively traced back to the extensive network of hydrogen bonds almost trapping the water molecules (see below). A similar behaviour has been already described, for example, in the case of the ApyH[Cu(N-sac)$_2$(O-sac)$(H_2O)_2$] species (ApyH = 2-aminopyridinium; sac = saccarinate),[12] showing one of the highest dehydration temperatures (396 K) for coordination compounds with *N,O*-pentacoordinated Cu^{II} ions.[13]

*$[Cu(Hoxonic)(bpy)_{0.5}]_n \cdot 1.5\,n\,H_2O$ (**2⊂H$_2$O**)*: The simultaneous thermal analysis performed on **2⊂H$_2$O** (Figure S1) revealed that, at 373 K, the compound undergoes an endothermic process ($\Delta H = 68.2\ kJ\,mol^{-1}$) interpreted, on the basis of the observed mass loss in the TG trace, as the complete removal of the clathrated water molecules to give the anhydrous form **2**. Water molecules loss upon moderate heating is consistent with the fact that they are not coordinated to

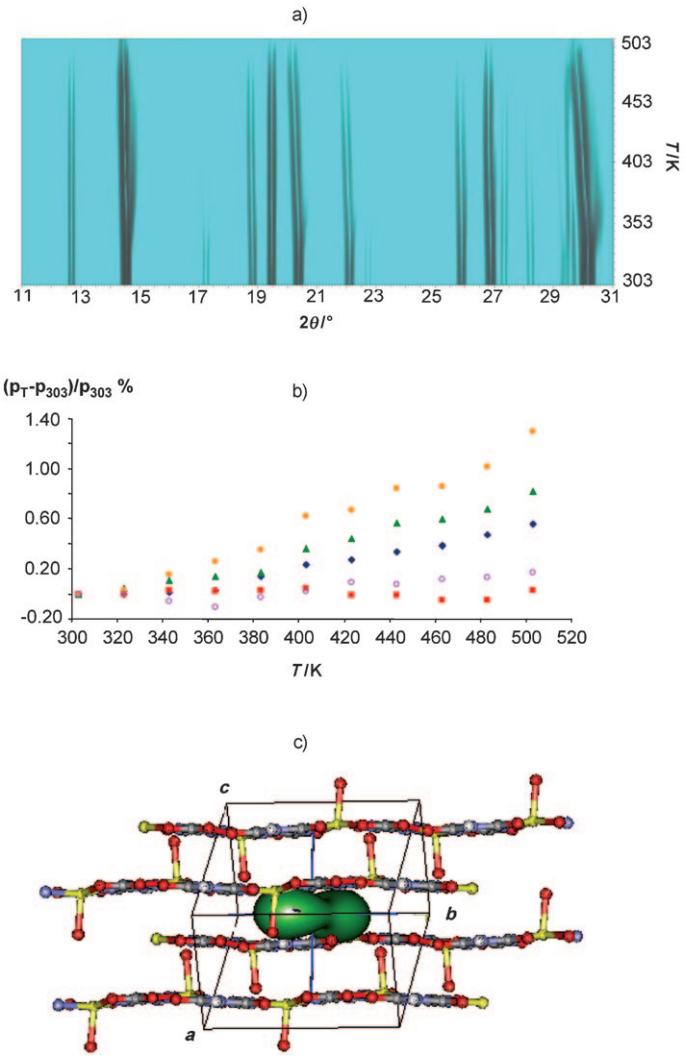

Figure 1. a) Variable-temperature X-ray diffractograms acquired on compound **1** in the 303–503 K temperature range. Horizontal axis, 2θ (°). Vertical axis, T (K). b) Variation of the unit cell parameters of **1** (p_T) normalised to the correspondent 303 K values (p_{303}), as a function of the temperature (a ◆; b ■; c ▲; β ○; V ●). c) Schematic drawing of the 1D chains in compound **1**. The graphical representation of the thermal strain tensor on passing form 303 to 503 K has been included.

the metal centres, yet weakly interact with the framework only by means of hydrogen bonds (see below). Compound **2** is stable until 543 K, temperature at which the decomposition process starts. The TXRPD experiments carried out in air on **2⊂H$_2$O** further strengthened these evidences (Figure 2).

The phase change from **2⊂H$_2$O** to **2** is fully reversible and proceeds without intermediates to the metastable anhydrous compound **2** in the form of a polycrystalline material of sufficient quality to allow a complete structural determination. Dehydration preserves the crystal system and the space group of the parent species, and promotes a moderate cell volume increase of about 1%. Further heating of **2** is accompanied by a negligible cell volume increase of less than 0.4%. On the whole, upon dehydration, the crystal structure

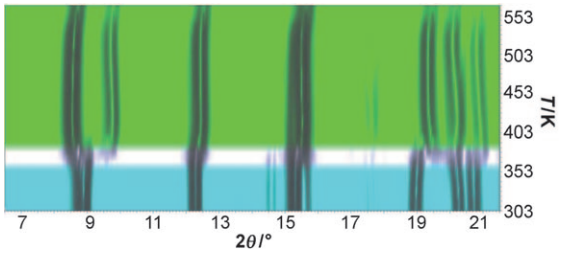

Figure 2. Variable-temperature X-ray diffractograms acquired for compound **2⊂H$_2$O** in the 303–563 K temperature range. Horizontal axis, 2θ (°); vertical axis, T (K). The white band indicates coexistence region of **2⊂H$_2$O** and **2** phases.

experiences a moderate rearrangement of the local structure (see below).

Crystal structures: The crystal structures of compounds **1**, **2⊂H$_2$O** and **2** were retrieved by means of ab initio X-ray powder diffraction methods (Table 1).

Table 1. Crystallographic data and details on the X-ray data collections and analyses for compounds **1**, **2⊂H$_2$O**, and **2**.

	1	**2⊂H$_2$O**	**2**
empirical formula	$C_4H_3CuN_3O_5$	$C_9H_8CuN_4O_{5.5}$	$C_9H_5CuN_4O_4$
M_r [g mol^{-1}]	236.63	323.73	296.71
crystal system	monoclinic	monoclinic	monoclinic
space group, Z	$P2_1/a$, 4	$C2/c$, 8	$C2/c$, 8
a [Å]	9.8506(4)	21.540(1)	22.886(4)
b [Å]	10.4359(5)	11.4662(7)	10.177(2)
c [Å]	6.3544(3)	9.3679(5)	10.098(1)
β [°]	105.948(2)	110.300(4)	114.43(1)
V [Å^3]	628.09(5)	2170.0(2)	2141.5(6)
ρ_{calcd} [g cm^{-3}]	2.48	1.96	1.84
$F(000)$	468	1304	1184
$\mu(Cu_{K\alpha})$ [cm^{-1}]	50.2	31.9	30.6
T [K]	298(2)	298(2)	393(2)
2θ range [°]	5–105	5–105	5–105
N_{data}	5001	5001	5001
N_{obs}	728	1258	1237
R_p, R_{wp} [a]	0.043, 0.064	0.099, 0.136	0.119, 0.161
R_{Bragg} [a]	0.052	0.045	0.030
V/Z [Å^3]	157	271	268

[a] $R_p = \Sigma_i\ |y_{i,o}-y_{i,c}|/\Sigma_i\ |y_{i,o}|$; $R_{wp} = [\Sigma_i\ w_i\ (y_{i,o}-y_{i,c})^2/\Sigma_i\ w_i\ (y_{i,o})^2]^{1/2}$; $R_{Bragg} = \Sigma_n\ |I_{n,o}-I_{n,c}|/\Sigma_n\ I_{n,o}$; $\chi^2 = \Sigma_i\ w_i\ (y_{i,o}-y_{i,c})^2/(N_{obs}-N_{par})$, for which $y_{i,o}$ and $y_{i,c}$ are the observed and calculated profile intensities, respectively, whereas $I_{n,o}$ and $I_{n,c}$ are the observed and calculated Bragg intensities. The summations run over i data points or n independent reflections. Statistical weights w_i are normally taken as $1/y_{i,o}$.

*[Cu(Hoxonic)(H$_2$O)]$_n$ (**1**)*: Compound **1** crystallises in the monoclinic $P2_1/a$ space group. The asymmetric unit is composed by one copper(II) ion, one Hoxonic ligand and one water molecule, all in general positions. The Cu^{II} metal centres are penta-coordinated and exhibit a slightly distorted square pyramidal stereochemistry of the CuN_2O_3 type: the pyramid base is defined by two nitrogen and two carboxylic oxygen atoms from two distinct Hoxonic ligands, adopting a *trans* disposition; the apical coordination position is occupied by the oxygen atom of one water molecule, protruding,

approximately along the [001] direction,[14] alternatively up and down with respect to the pyramid basal plane, and lifting the metal centre above it by 0.24 Å (Figure 1c). On the whole, the Hoxonic ligands adopt a tetradentate bischelate coordination mode, bridging adjacent metal centres 5.25 Å apart and yielding 1D polymeric chains built upon consecutive [Cu(Hoxonic)(H_2O)] monomers and running along [010]. The overall structural stability is enhanced by the formation of an extended net of hydrogen-bond interactions (in the 2.78-2.89 Å range), involving the water oxygen atoms and the triazine NH moieties and the oxygen atoms of adjacent chains.

*[Cu(Hoxonic)(bpy)$_{0.5}$]$_n$·1.5 n H_2O (**2**⊂**H_2O**) and [Cu(Hoxonic)(bpy)$_{0.5}$]$_n$ (**2**)*: Compound **2**⊂**H_2O** and its anhydrous form **2** crystallise in the monoclinic *C2/c* space group. The asymmetric unit is composed by one metal centre and one Hoxonic ligand in general positions, one bpy ligand lying about a crystallographic inversion centre (Wyckoff position *a*) and two water molecules, one in a general position and the other about a crystallographic two-fold axis (Wyckoff position *e*), giving a total of one and a half water molecules per asymmetric unit.

The Cu^{II} ions exhibit an octahedral stereochemistry of the *mer*-CuN_3O_3 kind, showing a non-negligible tetragonal distortion as a result of a pronounced Jahn–Teller effect. The Cu^{II} coordination sphere is defined by one nitrogen atom from a bpy ligand, by two *N,O*-chelating Hoxonic ligands, and by the carbonylic oxygen atom of a third Hoxonic moiety (Figure 3). Thus, in contrast to what is found in compound **1**, in **2**⊂**H_2O** and **2** the Hoxonic ligands adopt a pentadentate coordination mode, globally bridging three Cu^{II} ions, and promoting the formation of 2D corrugated layers growing orthogonally to [100]. The layers are pillared by the bpy ligands, along the symmetry related [410] and [4−10] directions, into a 3D framework possessing small isolated cavities, which, in the hydrated form, host the clathrated water molecules. The hosted water molecules are involved in hydrogen bond interactions (in the 2.61-2.87 Å range) with each other and with the triazine NH moieties and the carboxylic oxygen atoms of nearby Hoxonic moieties.

2⊂**H_2O** and **2** basically share similar structural features. Nevertheless, a closer look to their structures helps pointing out some subtle differences: Upon dehydration the system expands in the *ac* plane, while contracting along *b*, which consequently brings about an increase of the 2D layers corrugation. This implies a decrease of some of the Cu···Cu bridged distances. As a consequence, a relocation of both ligands takes place (Figure 3b): the Hoxonic moiety reduces its planarity, as witnessed by the dihedral angle between the triazine ring and the carboxylate group (2.18° and 12.86° in **2**⊂**H_2O** and **2**, respectively); the bpy moiety tilts its mean plane to fit the shorter Cu···Cu bridge.[15] Overall, the void volume left upon dehydration is about 12% of the unit cell volume.[16]

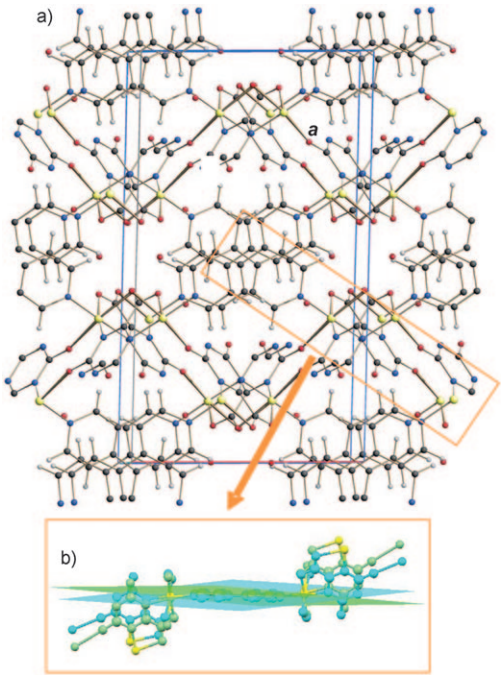

Figure 3. a) Schematic drawing, along [001], of the 3D framework of compound **2**⊂**H_2O**. Horizontal axis, *b*. Vertical axis, *a*. b) Comparison of the local structures of compounds **2**⊂**H_2O** and **2**. The root-mean-square planes of the two bpy ligands have been depicted to guide the eye.

Gas adsorption properties: The gas adsorption properties of **2** have been studied towards N_2 (77 K), CO_2 (195–363 K) and CH_4 (273–363 K). As described above, the structure of **2** contains small isolated cavities; therefore, in view of its structural features, this compound should not be considered as a porous material. In support of this, the N_2 isotherm performed at 77 K does not show any adsorption in the whole pressure range. Furthermore, CO_2 molecules are not incorporated in the framework at 195 K. However, the adsorption behaviour of **2** changes dramatically at higher temperatures with the CO_2 molecules being readily and reversibly incorporated in its framework at 273 K (up to 2.5 mmol g^{-1} at 2500 kPa, Figure 4).

It is also noteworthy that the behaviour of this system is guest selective, being able to incorporate only small

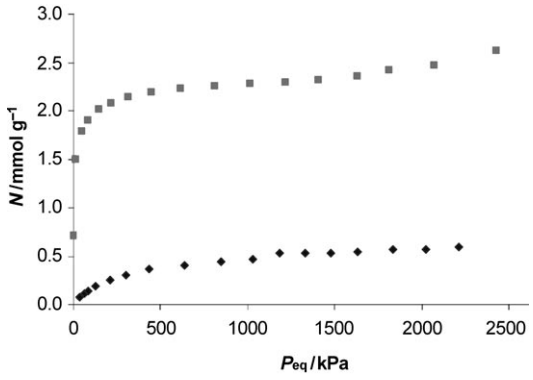

Figure 4. High pressure CH_4 (◆) and CO_2 (■) isotherms at 273 K for [Cu(Hoxonic)(bpy)$_{0.5}$]$_n$ (**2**).

amounts of CH_4 at 273 K and high pressure (up to 0.5 mmol g^{-1} at 2500 kPa) (Figure 4). A related CO_2/CH_4 selectivity has been previously found by us with the flexible $[M(5\text{-fluoropyrimidin-2-olate})_2]_n$ frameworks (M = Co, Zn), which was related to the polar nature of the pore windows favouring the incorporation of the quadrupolar CO_2 over apolar CH_4 guests.[8c] As mentioned above, **2** reversibly incorporates water molecules which is related to the polar nature of the cavities found in **2**. This feature should also contribute to its selectivity of quadrupolar CO_2 over apolar CH_4 guests. To further investigate the adsorptive properties of this system and in order to study the selectivity of **2** towards CO_2 over CH_4 we have performed variable-temperature zero coverage adsorption experiments and measurement of breakthrough curves of CO_2/CH_4 mixtures. Gas-phase adsorption experiments at low degrees of pore filling were studied by means of inverse gas chromatography (IGC) with a 15 cm column packed with pellets of **2** towards CO_2 and CH_4 in the temperature range 303 to 363 K.[17] The zero coverage experiments show that these gases do not follow the expected Henry's law behaviour. In the case of CO_2 this unusual behaviour can be observed above 323 K, whereas in the case of CH_4 the unusual behaviour is maintained in the whole temperature range studied (Figure S4). The lack of a porous structure in **2** and the fact that guest uptake and release is facilitated at higher temperatures suggest that the adsorption processes found in **2** are governed by the thermal energy of both a flexible framework and the kinetics energy of guest molecules. Indeed, guest molecules are only incorporated when the host possesses enough energy to breathe and the guest molecules have energy enough to diffuse through the host polar pockets. As a consequence of this, the ratio between CO_2 and CH_4 adsorption equilibrium constants decreases (1.17 to 1.05 log units) in the temperature range between 303 and 323 K and then monotonously increases with the temperature.

The differences in the adsorption equilibrium constants between CO_2 and CH_4 also suggested us the possible utility of **2** in the separation of CO_2/CH_4 mixtures. Indeed, measurements of breakthrough curves of a 0.5:0.5 and 0.05:0.95 (v/v) mixtures of CO_2/CH_4 flowed through a chromatographic column packed with **2** at 273 K show the passage of CH_4 through this material and the selective retention of CO_2 (Figure 5). In the case of an equimolecular mixture of CO_2/CH_4 the breakthrough takes place 270 s after dosing the gas mixture which represents 0.77 mmol of CO_2 being retained per gram of **2** under these dynamic conditions. Noteworthy, increasing the amount of CH_4 in the mixture to 95%, which corresponds to the typical composition of natural gas,[18] does not significantly change the performance of this material for CO_2 removal (Figure 5). Indeed, flowing a 0.05:0.95 (v/v) mixture of CO_2/CH_4 through the column packed with **2** indicates again the selective retention of CO_2 and the passage of CH_4 with breakthrough taking place after 1700 s, which indicates that 0.49 mmol of CO_2 have been retained per gram of **2** under these dynamic conditions. The diminution of the amount of CO_2 retained in the material upon enrichment with CH_4 of the gas mixture is a consequence of the diminution of the partial pressure of CO_2 in the gas mixture.

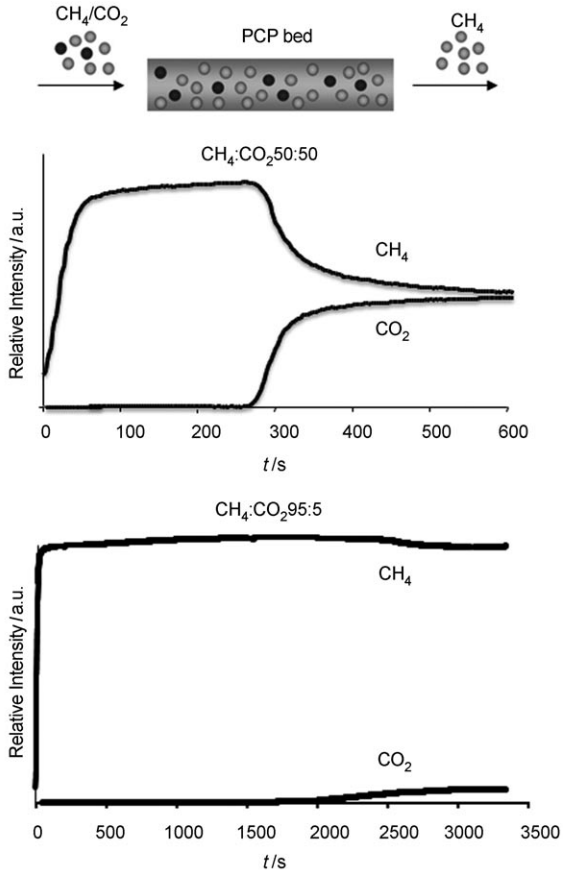

Figure 5. Schematic representation of the gas purification process and breakthrough curves of a stream of CH_4/CO_2 mixtures passed through a sample of **2** showing the retention of CO_2 and passage of CH_4. Top: equimolecular mixture of CH_4/CO_2. Bottom: 0.95:0.05 (v/v) mixture of CH_4/CO_2. The apparent diminution of the CH_4 signal after breakthrough is a consequence of composition dependence of ionisation in the gas mixture.

A similar selectivity has been found in ZIF-20[19] and in the amine functionalised MIL-53;[20] however, it should be noted that in the latter materials there is a highly accessible porous network. At variance, the crystal structure determinations of both **2**⊂H_2O and **2** show the existence of small isolated voids, which bring us to the conclusion of a dynamic behaviour of the flexible network of **2** upon exposure to polar guest molecules (H_2O, CO_2). In this regard, since the geometry and conformation of both Hoxonic and 4,4′-bpy ligands impose them a certain rigidity, the framework flexibility (dynamic behaviour) found in **2** is likely related to the typical plasticity of copper(II) coordination polyhedra.[21]

Conclusion

The oxonate system is able to efficiently bridge metal ions giving rise to the formation of the 1D system **1** which, upon

further reaction with the *N*,*N*′ spacer bpy, generates the 3D pillared structure of **2**. We have verified that the formation of this 3D material is favoured irrespectively of the reaction path used (i.e. conventional, solvent free, solid–solid and solid–liquid reaction).

In the case of **2**, it is also worth noting that, in spite of the lack of a porous structure, this material is able to readily and selectively incorporate guest molecules. This feature has been rationalised on the basis of the flexible response of the coordination network toward different probe gases at distinct temperatures. The results show that the adsorption phenomena in **2** are governed by the thermal energy of both the framework and the guest molecules and the polar nature of the voids in **2**. Indeed, the breakthrough experiments show the selective incorporation of quadrupolar CO_2 guest molecules from CH_4/CO_2 mixtures which is a process of industrial interest in order to enhance the combustion power of natural gas and to avoid pipeline corrosion.[18]

Experimental Section

Chemicals: all of the chemicals were of reagent grade and used as commercially obtained. The starting materials $\{[Cu(SiF_6)(4,4'bpy)_2]\cdot 8H_2O]\}_n$ and $\{[Cu(4,4'bpy)_2(H_2O)_2]\cdot SiF_6\}_n$ were prepared following the previously reported procedure.[11]

Synthesis of $[Cu(Hoxonic)(H_2O)]_n$ (1): An aqueous solution (20 mL) of $Cu(ClO_4)_2\cdot 6H_2O$ (2 mmol, 0.741 g) was added dropwise to an aqueous solution (30 mL) of oxonic acid potassium salt (2 mmol, 0.390 g) under stirring at 80 °C. After 3 h the resulting pale blue suspension was filtered and the solid obtained was washed with water, ethanol and diethyl ether. Yield: 68.5 %. Elemental analysis (%) calcd for $C_4H_3CuN_3O_5$: C 20.30, H 1.28, N 16.50; found: C 20.53, H 1.31, N 17.46.

Synthesis of $[Cu(Hoxonic)(bpy)_{0.5}]_n\cdot 1.5n\,H_2O$ ($2\supset H_2O$): We prepared compound $2\supset H_2O$ following four synthetic methods:

A water solution (20 mL) containing $Cu(CH_3COO)_2$ (2 mmol, 0.364 g) was added dropwise to oxonic acid potassium salt (2 mmol, 0.390 g) and 4,4′-bipyridine (1 mmol, 0.156 g) dissolved in 40 mL of water/ethanol (3:1) under stirring and heating at 80 °C. After 2 h the resulting suspension was filtered. The recovered powders were washed with water and ethanol, then dried with diethyl ether. Yield: 91 %. Elemental analysis calcd (%) for $C_9H_7CuN_4O_5$: C, 34.35; H, 2.24; N, 17.80; found: C, 31.86; H, 2.49; N, 16.29.

A mixture of $[Cu(Hoxonic)(H_2O)]_n$ (1 mmol, 0.219 mg) and 4, 4′-bipyridine (0.5 mmol, 78 mg) in 40 mL of water/methanol (15 mL:25 mL) was refluxed at 80 °C under stirring for two hours. The suspension was filtered and washed with water, ethanol and diethyl ether. Yield: 83 %.

A mixture of oxonic acid potassium salt (2 mmol, 390 mg) and $\{[Cu(SiF_6)(4,4'bpy)_2]\cdot 8H_2O]\}_n$ (0.5 mmol, 295 mg) was ground in an agate mortar during five minutes. The product was washed with acetone and dried. A light blue homogeneous powder was obtained. Yield: 100 %.

A mixture of oxonic acid potassium salt (0.4 mmol, 78 mg) and $\{[Cu(4,4'bpy)_2(H_2O)_2]\cdot SiF_6\}_n$ in water/ethylen glycol (1:3) was stirred at room temperature for 3 days. The suspension was filtered and washed with water, ethanol and diethyl ether. Yield: 100 %.

The nature and crystallinity of products obtained by routes 2–4 were verified by XRPD and the pattern was compared with that relative to compound $2\supset H_2O$ prepared as in method 1.

X-ray powder diffraction analysis: Polycrystalline samples of **1** and $2\supset H_2O$ were gently ground in an agate mortar, then deposited in the hollow of an aluminium sample holder equipped with a quartz monocrystal zero-background plate. The diffraction data were collected by using a θ:θ Bruker AXS D8 Advance vertical scan diffractometer equipped with a Ni-filtered CuKα ($\lambda = 1.5418$ Å) radiation, a linear position-sensitive Lynxeye detector, and with the following optics: primary Soller slits, 2.3°; divergence slit, 0.3°; receiving slit, 8 mm. The nominal resolution for the present set-up is 0.08° 2θ (FWHM of the α_1 component) for the LaB_6 peak at about 21.3° (2θ). The generator was operated at 40 kV and 40 mA. In the case of the metastable species **2**, the data were collected by using a Si monocrystal zero-background plate, at 393 K, by employing a custom-made, Peltier-controlled, sample heater (supplied by Officina Elettrotecnica di Tenno, Italy), and leaving all the other experimental conditions unaltered. For structure solution and refinement, overnight scans were performed in the 5–105° 2θ range, with $\Delta 2\theta = 0.02$°. For **1**, $2\supset H_2O$ and **2**, indexing by the single value decomposition approach,[22] as implemented in the TOPAS-R suite of programs,[23] allowed the determination of the crystal systems and of the lattice parameters, providing approximate unit cells (GOF = 55.5, 31.8 and 27.8 for $1\supset H_2O$, $2\supset H_2O$ and **2**, respectively), later refined by means of the Le Bail method. The space groups were assigned on the basis of the systematic absences. The structure solutions were initiated by the simulated annealing technique,[24] as implemented in TOPAS-R, using rigid Hoxonic and bpy fragments[25] and independent metal ions and water oxygen atoms. The final refinements were performed by the Rietveld method using TOPAS-R. The peak shapes were described by the fundamental parameters approach,[26] with the aid, when necessary, of a spherical harmonics description of the anisotropic full width at half maximum. The background was modelled by a polynomial function. An isotropic, refinable thermal parameter was assigned to the metal ions, augmented by 2.0 Å^2 for lighter atoms. A preferred orientation correction, in the March-Dollase formulation,[27] was introduced for **1** along the [001] pole. Scattering factors, corrected for real and imaginary anomalous dispersion terms, were taken from the internal library of TOPAS-R. A summary of the crystal data and refinement parameters, together with the profile and Bragg agreement factors, is supplied in Table 1. CCDC 737761 ($1\supset H_2O$), 737762 ($2\supset H_2O$) and 737763 (**2**) contain the supplementary crystallographic data for this paper. These data can be obtained free of charge from The Cambridge Crystallographic Data Centre via www.ccdc.cam.ac.uk/data_request/cif.

Thermodiffractometric measurements: A series of experiments was performed, to assess the thermal behaviour of the **1** and $2\supset H_2O$ phases, by employing a custom-made sample heater (supplied by Officina Elettrotecnica di Tenno, Italy), mounted on the Bruker AXS Advance D8 diffractometer. The compounds were manually grounded in an agate mortar and then deposited in the hollow of an aluminium sample holder. Typically, the thermodiffractometric experiments were planned on the basis of the STA results: A sequence of scans, in a significant, low-angle, 2θ range, was performed at 20 K per step, heating in situ from room temperature up to complete loss of crystallinity.[28]

Magnetism: Magnetic measurements were performed on polycrystalline samples by using a SQUID Quantum Design MPMS XL-5 (University of Granada) in the temperature range 2–300 K applying external fields of 5000 and 300 Oe.

Gas adsorption measurements: Adsorption isotherms were measured by using a Micromeritics Tristar 3000 (University of Granada) volumetric instrument. High-pressure adsorption isotherms were measured in a home-made volumetric adsorption instrument (University of Granada) equipped with two Baratron absolute pressure transducers (MKS type 627B). Their pressure ranges are from 0 to 133.33 kPa and from 0 to 3333.25 kPa, respectively, and the reading accuracy was 0.05 % of the usable measurement range. Prior to measurement, powder samples were heated at 403 K for 12 h and outgassed to 10^{-6} mbar.

Gas-phase adsorption at low degrees of pore filling was studied using the pulse chromatographic technique with a 15 cm column packed with 1.3 g of pellets of **2**. The sample was conditioned in He flow at 403 K for 12 h before the runs.

Gas separation experiments: The gas-separation property of **2** was examined by measurement of breakthrough curve experiments using CO_2/CH_4 gas mixtures (about 1:1 and 0.05:0.95 v/v) flowed through an activated sample of 1.3 g of pellets of **2** packed into a glass column (0.3 cm inner diameter ×15 cm length). Helium gas was initially purged into the

sample column. The column was cooled to 273 K using an ice bath. The gas mixture (100 kPa) was dosed into the column at a flow rate of 10 mL min^{-1}. The relative amounts of the gases passing through the column were monitored on a mass spectrometer gas analysis system (Pfeiffer vacoon) detecting ion peaks at m/z 44 (CO_2) and 16 (CH_4).

Acknowledgements

The authors acknowledge the financial support by Spanish Ministerium of Science and Innovation (CTQ2008-00037/PPQ) and the Fondazione CARIPLO (Project 2007-5117). G.T. thanks the Italian Ministero dell'-Università e della Ricerca for a doctoral grant (Progetto Giovani 2006 "Risparmio di Energia e Microgenerazione Distribuita"). E.B. and M.P.M. thanks MICINN for a Ramón y Cajal grant.

[1] See, for example, special issue on metal organic frameworks in *Chem. Soc. Rev.* **2009**, *38*, 1201–1508.
[2] See, for example, R. Matsuda, R. Kitaura, S. Kitagawa, Y. Kubota, R. V. Belosludov, T. C. Kobayashi, H. Sakamoto, T. Chiba, M. Takata, Y. Kawazoe, Y. Mita, *Nature* **2005**, *436*, 238–241.
[3] L. Alaerts, C. E. A. Kirschhock, M. Maes, M. A. van der Veen, V. Finsy, A. Depla, J. A. Martens, G. V. Baron, P. A. Jacobs, J. F. M. Denayer, D. E. De Vos, *Angew. Chem.* **2007**, *119*, 4371–4375; *Angew. Chem. Int. Ed.* **2007**, *46*, 4293–4297.
[4] See for example, a) Z. Wang, G. Chen, K. Ding, *Chem. Rev.* **2009**, *109*, 322–359; b) F. Gándara, E. Gutierrez-Puebla, M. Iglesias, D. M. Proserpio, N. Snejko, M. A. Monge, *Chem. Mater.* **2009**, *21*, 665–661.
[5] See for example, a) S. Kitagawa, K. Uemura, *Chem. Soc., Rev.* **2005**, *34*, 109–119; b) S. Devautour-Vinot, G. Maurin, F. Henn, C. Serre, T. Devic, G. Ferey, *Chem. Commun.* **2009**, 2733–2735.
[6] S. Takamizawa, M. Kohbara, R. Miyake, *Chem. Asian J.* **2009**, *4*, 530–539.
[7] N. Masciocchi, S. Galli, A. Sironi, E. Cariati, M. A. Galindo, E. Barea, M. A. Romero, J. M. Salas, J. A. R. Navarro, F. Santoyo-González, *Inorg. Chem.* **2006**, *45*, 7612–7620.
[8] See for example, a) J. A. R. Navarro, E. Barea, A. Rodríguez-Diéguez, J. M. Salas, C. O. Ania, J. B. Parra, N. Masciocchi, S. Galli, A. Sironi, *J. Am. Chem. Soc.* **2008**, *130*, 3978; b) G. Beobide, W.-G. Wang, O. Castillo, A. Luque, P. Román, U. García-Couceiro, J. P. García-Terán, G. Tagliabue, S. Galli, J. A. R. Navarro, *Inorg. Chem.* **2008**, *47*, 5267–5277; c) S. Galli, N. Masciocchi, G. Tagliabue, A. Sironi, J. A. R. Navarro, J. M. Salas, L. Mendez-Liñan, M. Domingo, M. Perez-Mendoza, E. Barea, *Chem. Eur. J.* **2008**, *14*, 9890–9901.
[9] a) J. A. R. Navarro, E. Barea, J. M. Salas, N. Masciocchi, S. Galli, A. Sironi, J. B. Parra, C. O. Ania, *Inorg. Chem.* **2006**, *45*, 2397–2399; b) J. A. R. Navarro, E. Barea, J. M. Salas, N. Masciocchi, S. Galli, A. Sironi, C. O. Ania, J. B. Parra, *J. Mater. Chem.* **2007**, *17*, 1939–1946.
[10] S. A. Barnett, N. R. Champness, *Coord. Chem. Rev.* **2003**, *246*, 145–168.
[11] S. Noro, R. Kitaura, M. Kondo, S. Kitagawa, T. Ishii, H. Matsuzaka, M. Yamashita, *J. Am. Chem. Soc.* **2002**, *124*, 2568–2583.
[12] V. T. Yilmaz, F. Yilmaz, *Transition Met. Chem.* **2005**, *30*, 95–102.
[13] Although the moderately stable trigonal bipyramidal stereochemistry of its copper(II) ions partially counterbalance the stability of the coordinated water molecules.
[14] Notably, this is consistent with the [001] pole of the March–Dollase preferred orientation correction applied during the Rietveld refinement stage.
[15] Dehydration promotes shortening of some bridged Cu···Cu vectors (Hoxonic bridge: 5.48 versus 5.46 Å; bpy bridge: 11.08 versus 10.98 Å, this bringing about a relocation of the Hoxonic and bpy ligands.
[16] PLATON, A. L. Spek, *J. Appl. Crystallogr.* **2003**, *36*, 7–13.
[17] a) M. C. Almazán-Almazán, M. Pérez-Mendoza, I. Fernández-Morales, M. Domingo-García, F. J. López-Garzón, *J. Chromatogr. A* **2008**, *1190*, 271–277; b) M. Pérez-Mendoza, M. C. Almazán-Almazán, L. Méndez-Liñán, M. Domingo-García, F. J. López-Garzón, *J. Chromatogr. A* **2008**, *1214*, 121–127.
[18] Y.-S. Bae, K.-L. Mulfort, H. Frost, P. Ryan, S. Punnathanam, L. J. Broadbelt, J. T. Hupp, R. Q. Snurr, *Langmuir* **2008**, *24*, 8592–8598.
[19] H. Hayashi, A. P. Côté, H. Furukawa, M. O'Keeffe, O. M. Yaghi, *Nat. Mater.* **2007**, *6*, 501–506.
[20] S. Couck, J. F. M. Denayer, G. V. Baron, T. Remy, J. Gascon, F. Kapteijn, *J. Am. Chem. Soc.* **2009**, *131*, 6326–6327.
[21] E. Barea, J. A. R. Navarro, J. M. Salas, N. Masciocchi, S. Galli, A. Sironi, *J. Am. Chem. Soc.* **2004**, *126*, 3014–3015.
[22] A. A. Coelho, *J. Appl. Crystallogr.* **2003**, *36*, 86–95.
[23] Topas-R: General profile and structural analysis software for powder diffraction data; Bruker AXS, Karlsruhe, **2001**.
[24] A. A. Coelho, *J. Appl. Crystallogr.* **2000**, *33*, 899–908.
[25] Hoxonic: C-C=C-N = 1.39 Å, C–C(O) = 1.45 Å, C–O = 1.35 Å, C=O = 1.25 Å, aromatic ring angles = 120°. The bpy fragment was found in the Cambridge Structural Database.
[26] R. W. Cheary, A. A. Coelho, *J. Appl. Crystallogr.* **1992**, *25*, 109–121.
[27] a) A. March, *Z. Kristallogr.* **1932**, *81*, 285–297; b) W. A. Dollase, *J. Appl. Crystallogr.* **1987**, *20*, 267–272.
[28] Note: The absolute temperature values detected during the TXRPD experiments may differ from those observed by the STA measurements. A thermal gradient exists between the temperature measured by the thermo couple of the TXRPD chamber and the actual temperature of the sample, the temperature values measured by the STA apparatus thus being more reliable.

Received: August 25, 2009
Published online: November 24, 2009

